Biomechanics Open Library

Original Research Article | Open Access

Increase in vibration following vertebral endplate fracture: Potential for endplate fracture detection

[1]Matthew C. Coombs,[*] [1]Kermit G. Davis , [1]Susan E. Kotowski, [2,3]Robert J. Parkinson, [2]Jack P. Callaghan

[1] University of Cincinnati, Cincinnati, OH, USA
[2] University of Waterloo, Waterloo, ON, Canada
[3] Giffin Koerth Forensics, Toronto, ON, Canada

[*]**Corresponding Author:** Kermit Davis, University of Cincinnati, Cincinnati, OH, USA, Phone: 513-558-2809 , Email: kermit.davis@uc.edu

Edited by: Prof. Vytautas Ostasevicius, Director of Mechatronics Institute, Kaunas University of Technology, Kaunas, Lithuania Email: vytautas.ostasevicius@ktu.lt, Ehsan Masoumi Khalil Abad, Mechanical Engineering Department, McGill University, Montreal, Quebec, Canada. ehsan.masoumikhalilabad@mail.mcgill.ca, Morshed Khandaker, PhD, Associate Professor, Department of Engineering and Physics ,University of Central Oklahoma, Email:mkhandaker@uco.edu

Keywords: Vertebral endplate fracture; spine; vibration; structural health monitoring; cyclic loading; vibration; axial deformation; cumulative loading; force-deformation; functional spine unit

Received: August 07, 2015 **Accepted:** October 30, 2015 **Published:** November 18, 2015

Abstract

Traditionally, *in vitro* intervertebral joint failure identification has been limited to observation of gross decreases in motion segment height, changes in force-deformation response, and post-test dissection. The purpose of this study was to determine whether changes in vibration transfer through the intervertebral joint could be used to accurately identify the loading cycle in which the vertebral endplate fractured. Fifteen functional spinal units were loaded in a pattern mimicking repetitive lifting with intermittent heel strikes, until fracture was believed to have occurred. Specimen axial deformation and vibration were measured. Following testing, specimens were dissected and vertebral endplate fractures were classified, and grouped as either detected fracture or non-detected fracture based upon whether or not maximum vibration exceeded 1.5x baseline vibration. For the fracture group, peak vibration increased 1222% ($p<0.0001$) from 4.65 m/s^2 (±4.26) at baseline to a maximum of 61.51 m/s^2 (±34.86). Non-detected fracture specimens showed minimal increases in vibration response, with peak vibration increasing 26% ($p<0.10$). Vibration analysis using structural health monitoring techniques may be useful to determine the occurrence of vertebral endplate fractures *in vitro*, and may lead to insights into fracture development and propagation.

Introduction

One pathway for intervertebral disc degeneration is an injury cascade beginning with damage to the vertebral endplates resulting in changes to the loading and nutrient flow of the intervertebral disc [1,2,9,29]. Vertebral endplate damage is likely common, given the prevalence of micro-fractures and healing trabeculae found in most cadaveric vertebral bodies [32]. Vertebral endplate damage, observed as endplate fractures, has been shown to increase with both cumulative loading and the magnitude of applied load [4, 26], and exposure to whole body vibration [24,28,33]. Individuals who experience increased loading doses through regular engagement in manual materials handling tasks [14,19], whole body vibration, or individuals with diminished bone density or quality [8,10,13,20,21], may be at elevated risk for vertebral endplate fractures.

In vitro biomechanical testing has been used to study intervertebral joint strength, durability, and injury mechanisms leading to vertebral endplate damage. However *in vitro* testing is limited by the inability to identify the specific cycle of injury occurrence within a cumulative (cyclic) loading protocol, and injury classification can typically only be done at the conclusion of the biomechanical test protocol. The traditional approach to identifying vertebral fractures *in vitro* relies upon reductions in motion segment height, changes in force-deformation response and post-test dissection [2,25]. Only recent studies have started to include energy transfer through the structure of the intervertebral joint as a response to loading during *in vitro* biomechanical testing [11,16,17]. Structural health monitoring techniques study the vibration response of the intervertebral joint to applied loads, which provides information on material properties and joint integrity [7,12]. It may be that changes in vibration may identify injury to the intervertebral joint during *in vitro* biomechanical testing, and potentially link loading cycle to endplate fracture occurrence.

Already, structural health monitoring techniques have been demonstrated to be highly reliable in the detection of changes in some intervertebral joint properties *in vitro* [11,16,17]. It has been reported that low back injury reduces the shock absorption capacity of the intervertebral joint by as much as 30% [32], therefore, changes in vibration after injury may be large. In this manner analysis of the time history of vibration response of biological structures may be an effective tool to identify the initiation of damage events to the intervertebral joint during prolonged *in vitro* biomechanical testing.

Implementing structural health monitoring techniques for the *in vitro* study of the most basic intervertebral joint unit under loading conditions may provide insights into fracture development and propagation. Current methods lack the ability to identify the cycle of fracture occurrence or changes in force transmission through the intervertebral joint leading up to fracture occurrence. Additionally, including these simple structural health monitoring

techniques may provide clarity to the reporting of gross biomechanical changes during testing. The purpose of this study was to determine whether structural health monitoring techniques, specifically changes in vibration during loading, could identify vertebral endplate fractures *in vitro*, as well to classify such fractures, and to potentially identify initiation of micro-fracture development.

Materials & Methods

Nine porcine cervical spines from animals that were approximately six months old with a mean weight of 80 kg, were harvested immediately postmortem. Spines were immediately frozen at -20 °C, and stored until use. Prior to testing, spines were thawed at room temperature for 12-15 hours, and dissected into functional spinal units (FSUs) consisting of eight C3-4 and seven C5-6 units (n=15). All muscle tissue was removed, leaving the osteoligamentous structure intact. After dissection, vertebrae were potted in aluminum cups using non-exothermic dental stone (Denstone®; Miles Inc., South Bend, IN). Instrumented specimens were mounted to a servo-hydraulic materials test system (Instron 8872, Instron, Norwood, MA), oriented with the axis of compression (Figure 1). Specimens were instrumented with four tri-axial accelerometers (Series 2 Accelerometers, NexGen Ergonomics, Quebec, Canada), with one accelerometer placed on the posterior surface of the cephalad vertebral body, one on the anterior surface of the cephalad vertebral body, and another two on the caudad vertebral body (Figure 2). Accelerometers provided continuous measurement of vibration, recorded at 1024 Hz. The high sampling rate is set by the instrumentation for the purpose of vibration analysis, and is common for structural health monitoring techniques.

Cyclic compressive loads were applied with an initial peak magnitude of 4 kN, at a rate of 2 Hz. After every 100 cycles, a 1.5 kN impulse load was applied which are standard levels that correspond to typical lifting conditions in the workplace. After 200 impulses, cyclic load magnitude was increased by 1 kN. This loading pattern was repeated until fracture was believed to have occurred due to audible fracture or significant height loss as measured by the Instron system (Figure 3). Loading was designed to mimic lifting, with intermittent impulse load magnitudes similar to heel strikes [3,26]. Specimen axial deformation and compressive force were measured from the materials test system crosshead displacement and load cell, respectively, each recorded at 100 Hz.

A custom MATLAB (MATLAB R2011b, The MathWorks, Inc., Natick, MA) program was used to process load, displacement, and vibration magnitude. A 23rd order polynomial was fit to displacement, which was the lowest order, well-conditioned polynomial to fit the displacement results. For each specimen, baseline and maximum vibration were recorded. Baseline vibration was defined as the maximum vibration magnitude of the first twenty cycles, prior to the first impulse, from the peak accelerometer. Maximum vibration was defined as the maximum magnitude vibration recorded during the entire test across all accelerometers. Each specimen served as its own control, comparing maximum vibration response to baseline response. Specimens were classified as either detected fracture or non-detected frac-

Figure 1: Biomechanical test setup for cyclic compression.

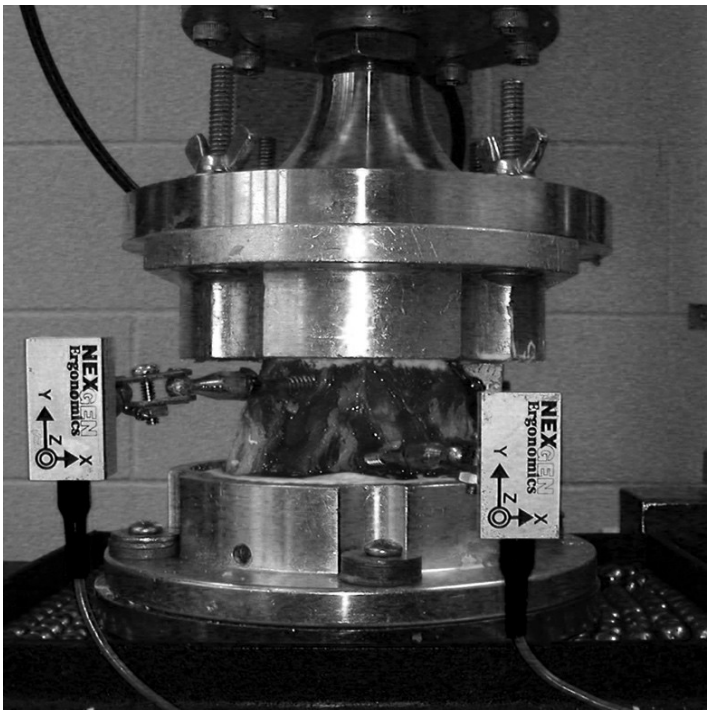

Figure 2: Functional spinal unit mounted in aluminum cups and connected to materials test system. Specimen is instrumented with tri-axial accelerometers, prepared for cyclic compression.

ture, based upon whether or not maximum vibration exceeded 1.5x baseline vibration, respectively. It was felt by the authors that the 1.5x threshold value was significantly large enough for this pilot study to remove signal artifacts, while still small enough to provide sensitivity to changes in system connectivity.

Following biomechanical testing, specimens were dissected with an incision through the disc, and the vertebral bodies were separated. After drying for 24-48 hours, visual inspection of the vertebral endplates was performed to identify vertebral endplate fractures. Vertebral endplate fractures were classified as stellate, lateral, anterior-posterior, ring, or soft/spongy endplate [4,16].

Mean percent change in vibration magnitude, grouped by fracture classification, was calculated as change from baseline vibration normalized to baseline vibration. Differences between baseline and maximum vibration were determined by one-tailed paired t-tests (α=0.05) for detected and non-detected fracture groups (Excel, Microsoft, Redmond, CA), with each specimen serving as its own control. Differences between fracture classifications of maximum vibration for the fracture group were determined by one-way ANOVA (α=0.05).

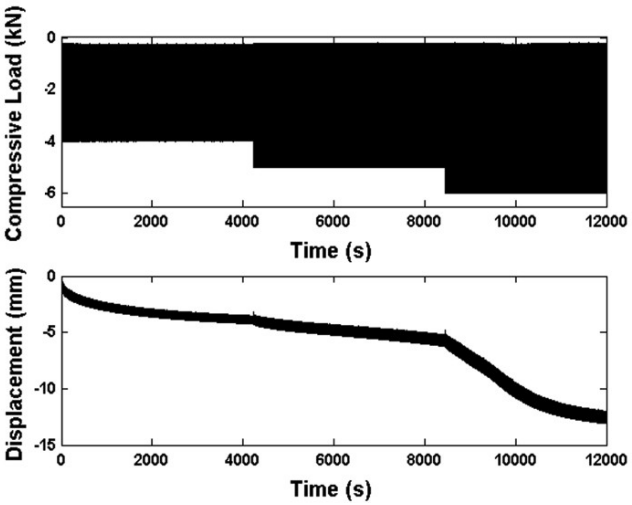

Figure 3: Loading profile applied to specimen (top), with resulting specimen compression (bottom). Selected specimen, Spine 1 C3-C4, was classified as fractured by the threshold criteria.

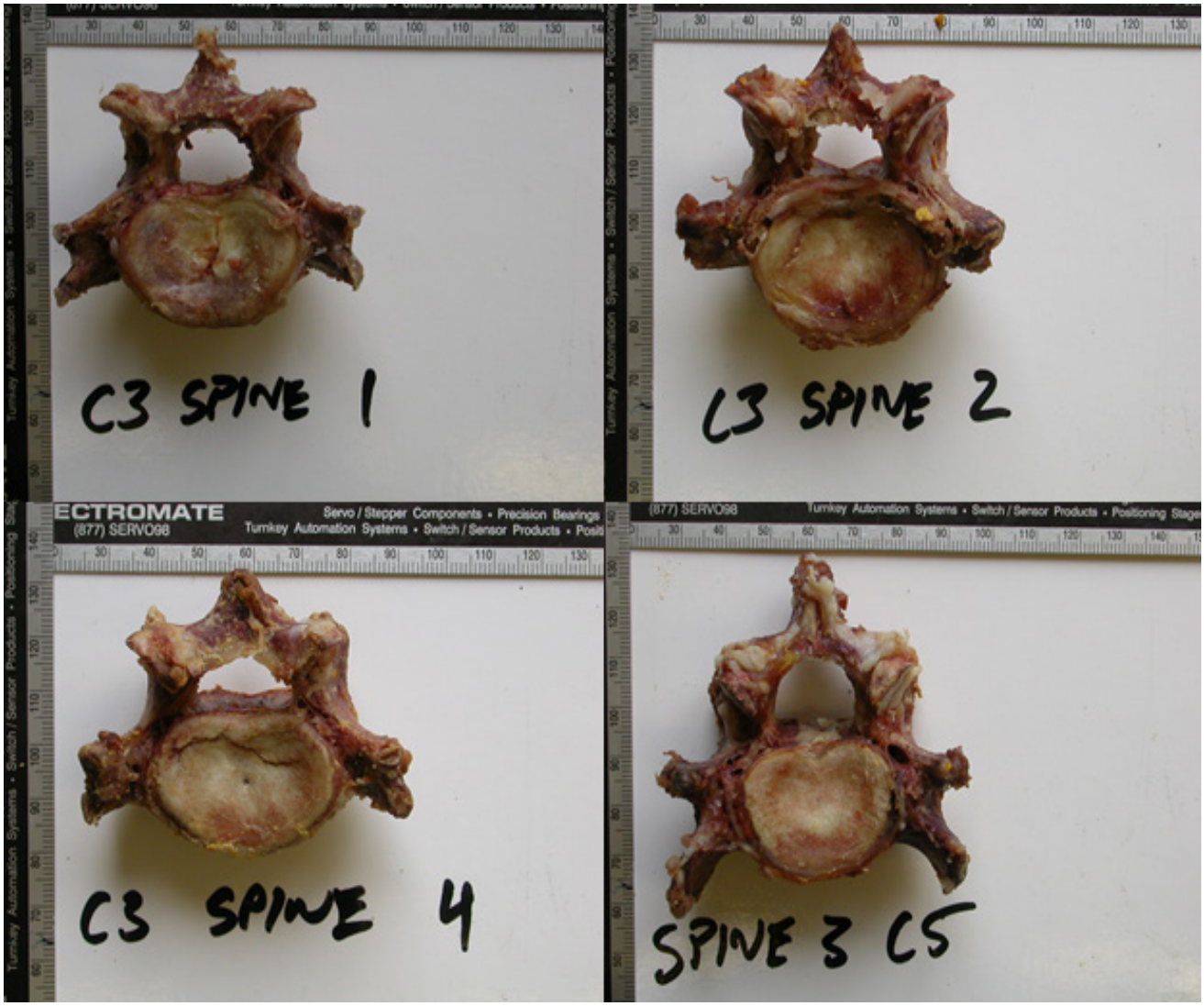

Figure 4: Photographs of vertebral endplate fractures after dissection and drying. Top Left: AP Fracture located mid-body. Top Right: Ring fracture on right lateral aspect. Bottom Left: Lateral fracture located on the posterior aspect. Bottom Right: Soft-spongy endplate fracture located in the center of the specimen.

Results

Eleven of fifteen specimens met the fracture threshold criteria of a 1.5x increase in vibration magnitude. All specimens classified as fractured by the threshold criteria possessed vertebral fractures upon dissection (Table 1 and Figure 4). In the fracture group, there were two anterior-posterior fractures, four ring fractures, five lateral fractures, and one soft/spongy endplate fracture. One specimen in the fracture group had both an anterior-posterior fracture and a lateral fracture, on adjacent vertebrae. All other specimens in the fracture group only had one fracture type. Four specimens did not meet the threshold criteria, and were classified as non-detected fracture. Following dissection, in the non-detected fracture group there was one anterior-posterior fracture, one ring fracture and two soft/spongy endplate fractures. In the non-detected fracture group, specimens classified as possessing soft/spongy endplate fractures, had no obvious fracture lines, and were classified based on the 'whiteness' of the vertebral endplate suggesting that underlying trabecular was damaged. One specimen, Specimen 6 C3-C4, grouped in the non-detected fracture group had only minor fracturing of the vertebral endplate. Only one specimen, Specimen 7 C3-C4, possessed a significant vertebral AP endplate fracture mid-body, but did not meet the threshold criteria.

Specimens classified as fractured all demonstrated a change from low level baseline vibration, to an increased broadband response following hypothesized fracture occurrence (Figure 5). For specimens classified as fractured, maximum vibration was 1222% higher than baseline vibration, increasing by 12 times ($p<0.0001$) from 4.65 m/s^2 (±4.26) to 61.51 m/s^2 (±34.86) (Figure 6). Non-detected fracture specimens showed minimal increases in vibration, increasing 26% ($p<0.10$) from 7.71 m/s^2 (±7.37) at baseline to a maximum of 9.68 m/s^2 (±6.19). There was no difference ($p<0.96$) in maximum vibration between fracture types (Figure 7).

Qualitative changes in deformation were determined for specimens meeting the threshold criteria. Specimens meeting the fracture threshold criteria all demonstrated a sharp increase in displacement during testing (Figure 8). For the fracture group, sharp increases in displacement occurred at similar time points as the occurrence of vibration response magnitude first exceeding the threshold criteria. Non-detected fracture specimens showed a slow increase in displacement over the duration of the test.

		Primary Fracture Classification	Secondary Fractures
Detected Fracture	**Specimen# 1, C3-C4**	AP fracture mid-body on C3	Soft/spongy endplate on mid-to-left lateral aspect of C4
	Specimen# 2, C3-C4	Ring fracture on right lateral aspect of C3	None
	Specimen# 2, C5-C6	Ring fracture on anterior aspect of C5	Ring fracture on anterior aspect of C6
	Specimen# 3, C3-C4	Ring fracture on right-posterior aspect of C3	None
	Specimen# 4, C3-C4	Lateral fracture on posterior aspect of C3	Soft/spongy endplate on posterior aspect of C4
	Specimen# 4, C5-C6	Soft spongy endplate on C5	None
	Specimen# 7, C5-C6	AP fracture mid-body, with crushing on C5	Lateral fracture on posterior aspect, followed by significant crushing on C6
	Specimen# 8, C3-C4	Ring fracture on posterior, left lateral aspect on C3	None
	Specimen# 8, C5-C6	Lateral fracture mid-body on C5	Lateral fracture mid-body on C6
	Specimen# 9, C3-C4	Lateral fracture on posterior aspect on C3	Lateral fracture mid-body on C4
	Specimen# 9, C5-C6	Lateral fracture mid-body on C5	None
Non-Detected Fracture	**Specimen# 3, C5-C6**	Soft spongy endplate on C5	Soft spongy endplate on mid-to-left lateral aspect of C6
	Specimen# 5, C5-C6	Soft spongy endplate on C5	Soft spongy endplate on C6
	Specimen# 6, C3-C4	Ring fracture on left posterior aspect on C3	Ring fracture on left posterior aspect on C4
	Specimen# 7, C3-C4	AP fracture mid-body on C3	None

Table 1: Vertebral endplate fracture classifications for Detected Fracture group and Non-Detected Fracture group

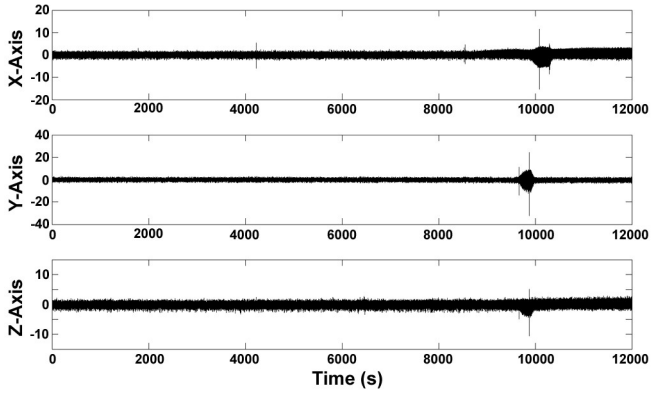

Figure 5: Vibration response of representative specimen(Spine 1 C3-C4, same as Figure 3) during cyclic loading.

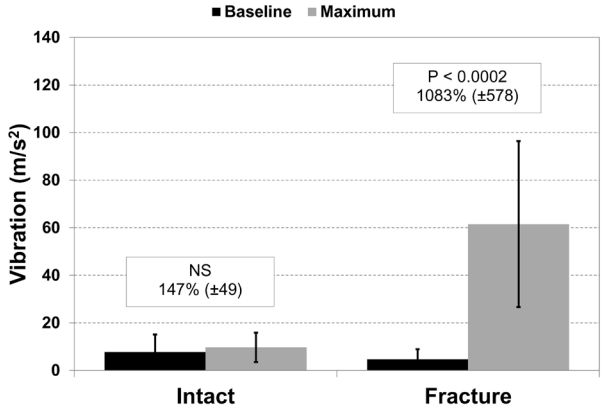

Figure 6: Mean baseline and maximum vibration response for intact and fracture groups.

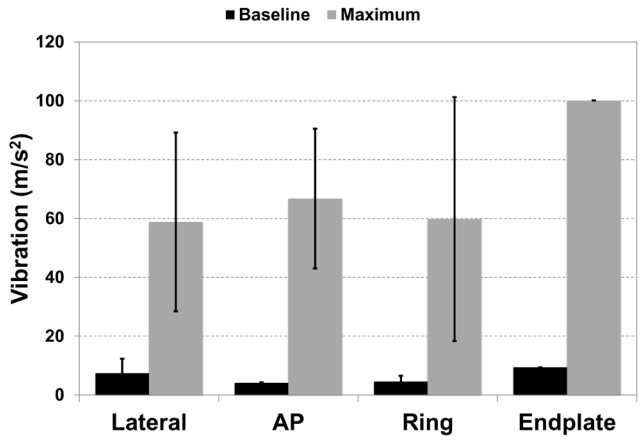

Figure 7: Mean baseline and maximum vibration response for fracture group, categorized by fracture type.

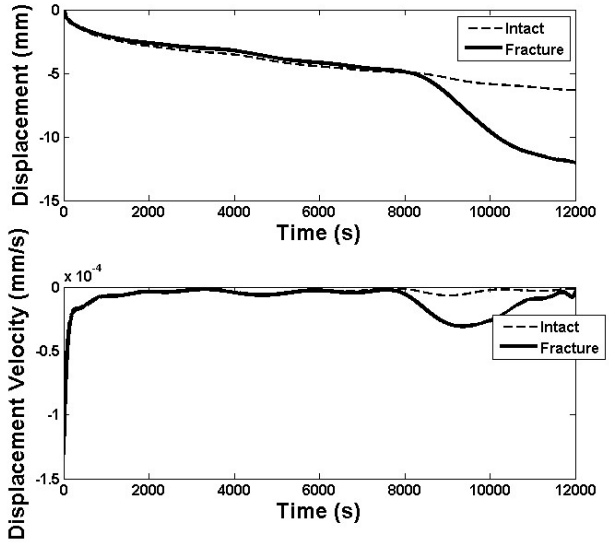

Figure 8: Specimen displacement and velocity for intact (dotted) and fractured (solid) specimens. Fractured specimen same as Figures 3 and 5.

Discussion

Clear differences were determined in vibration and displacement responses between specimens classified as detected and non-detected fracture. Specimens meeting the threshold criteria experienced a large increase in vibration magnitude and specimen displacement following endplate fracture, with average maximum vibration more than twelve times baseline. Specimens with no detected fracture showed smaller, insignificant increases in baseline vibration and displacement for the duration of testing. Endplate fractures were found in all specimens, with primarily ring and lateral fractures in specimens classified as fractured, and primarily soft/spongy endplate fractures in specimens classified as non-detected fracture. There was no difference in maximum vibration between fracture classifications in the fracture group, limited by large variation within individual fracture types.

The main limitation with this study is the small sample size, which limited the scope of the comparisons able to be made by this preliminary study. However, the small sample size does not directly affect the results or conclusions of this study. With more specimens it may be possible to explore the sensitivity of vibration response to the type and severity of endplate fractures. Our study protocol did not include radiographic analysis before and after biomechanical testing, and it is possible that some changes in vibration are due to non-detected changes in specimen internal structure. However specimens were taken from young, healthy porcine tissue in order to minimize pre-existing specimen defects prior to testing. Due to the long duration of each test, considerable changes in viscoelastic response of the intervertebral joint are expected. Disc hydration over several hours under large compressive loads would be expected to result in drying of the intervertebral disc, altering vibration response. However, this method is focused on changes in vibration magnitude, rather than specific changes in vibration through the joint. In addition, every attempt was made to preserve normal disc hydration during testing, and the magnitude of change in the detected fracture group cannot be fully explained by marginal intervertebral disc dehydration. Minimization of dehydration was accomplished by having specimens remain in enclosed bag until testing, and minimizing the time between freezer and testing. As we did not record the time at which audible fracture occurred during testing, we were unable to relate the time at which the fracture threshold criteria was first met to the loading cycle associated with specimen failure. In addition, the fracture threshold criteria used in this study was not based upon any physiologic parameter and has not been previously studied. It is unknown how sensitive increases in vibration are to changes to the structure of the intervertebral joint; however, results from this study suggest that vibration magnitude is sensitive to small changes in the integrity of the intervertebral joint, closely matching changes in load-deformation response. Additional work is required to properly define the fracture threshold criterion corresponding to exact cycle of injury.

It was considered that accelerometer placement into the vertebral bodies may alter baseline structural health of specimens, however in no specimen was the fracture observed to propagate through the endplate into the defect created from accelerometer installation. Rigid potting was also employed which can significantly alter the natural boundary conditions of the specimen. The use of porcine cervical spines, and the subsequent differences between human and porcine joint anatomy and material properties, is expected to be secondary to changes in vibration before and after vertebral endplate fracture. Domestic swine have been used as models for the adolescent and adult human spine, due to similar vertebral body size, geometry, regional mechanical properties and cancellous microarchitecture [5,18,30,31,36]. Despite differences in gait and anatomic orientation during daily activity, similarities in compressive properties between quadrupedal and bipedal spines *in vivo* have been reported [6,22,23,27,35]. One key limitation in using porcine vertebrae in this study is porcine vertebral bone density is about double that of humans [31], which may impact rate of vibration transmission. However, animal models are beneficial for normalizing joint health prior to testing in comparison to cadaveric tissue.

To date, it has not been possible to determine why some specimens did not meet the vibration threshold criteria, despite having significant endplate fractures. Correct classification by this method *in vitro* may be further limited by the ability to precisely stop the test close to fracture occurrence. In many specimens, in addition to the primary fracture, other minor endplate and specimen defects were evident. It is possible that following initial fracture, additional load cycles resulted in secondary fractures and damage to the underlying trabeculae. Prior to specimens meeting the threshold criteria, small increases in vibration were observed, hypothesized to occur as the result of micro-fracture

development and propagation before ultimate endplate failure.

In conclusion, changes in vibration response of functional spinal units to moderate compressive and impulse loading appeared related to the presence of vertebral endplate fractures *in vitro*. Following additional evaluation of this methodology, vibration response changes may be an additional tool for the *in vitro* quantification of changes to functional spinal units. The conclusions of this study however are preliminary, and more work is needed to develop a controlled test protocol to quantify the relationship between changes in vibration to changes in intervertebral joint health in the periods before, leading up to and after fracture. The current work is only the first step in understanding how the mechanical properties of the vertebral endplate change in response to loading and the occurrence to failure. A large study that investigates the vibration response to different types of fractures may identify unique signatures (e.g. changes in different directions).

References

[1] Adams MA, Freeman BJ, Morrison HP, et al. Mechanical initiation of intervertebral disc degeneration. Spine 2000;25(13):1625–36.

[2] Adams MA, McNally DS, Wagstaff J, et al. Abnormal stress concentrations in lumbar intervertebral discs following damage to the vertebral bodies: a cause of disc failure? Eur Spine J 1993;1(4):214-21.

[3] Bhattacharya A, Watts NB, Davis KG, et al. Dynamic bone quality: a non-invasive measure of bone's biomechanical property in osteoporosis. J Clinical Densitom 2010;13(2):228–36.

[4] Brinckmann P, Biggemann M, Hilweg D. Fatigue fracture of human lumbar vertebrae. Clinical Biomech 1988;3 Suppl 1:i–S23.

[5] Busscher I, van der Veen AJ, van Dieën JH, et al. In vitro biomechanical characteristics of the spine: a comparison between human and porcine spinal segments. Spine 2010;35(2):E35–42.

[6] Bylski-Austrow DI, Glos DL, Sause FE, et al. In vivo dynamic compressive stresses in the disc annulus: a pilot study of bilateral differences due to hemiepiphyseal implant in a quadruped model. Spine 2012;37(16):E949–56.

[7] Carden EP and Fanning P. Vibration based condition monitoring: a review. Structural Health Monitoring 2004;3(4):355–77.

[8] Cody DD, Goldstein SA, Flynn MJ, et al. Correlations between vertebral regional bone mineral density (rBMD) and whole bone fracture load. Spine 1991;16(2):146–54.

[9] van Dieën JH, Weinans H, Toussaint HM. Fractures of the lumbar vertebral endplate in the etiology of low back pain: a hypothesis on the causative role of spinal compression in aspecific low back pain. Med Hypotheses 1999;53(3):246–52.

[10] Duan Y, Parfitt AM, Seeman E. Vertebral bone mass, size, and volumetric density in women with spinal fractures. J Bone Miner Res 1999;14(10):1796–1802.

[11] van Engelen SJ, van der Veen AJ, de Boer A, et al. The feasibility of modal testing for measurement of the dynamic characteristics of goat vertebral motion segments. J Biomech 2011;44(8):1478–83.

[12] Farrar CR and Worden K. An introduction to structural health monitoring. Philo Trans A Math Phys Eng Sci 2007;365(1851):303–15.

[13] Ferguson SJ and Steffen T. Biomechanics of the aging spine. Eur Spine J 2003;12(Suppl 2):S97–103.

[14] Genaidy AM, Waly SM, Khalil TM, et al. Spinal compression tolerance limits for the design of manual material handling operations in the workplace. Ergonomics 1993;36(4):415–34.

[15] Gallgher, S, W S Marras, A S Litsky, D Burr. 2005. "Torso flexion loads and the fatigue failure of human lumbosacral motion segments." Spine 30(20): 2265-2273.

[16] Kawchuk GN, Decker C, Dolan R, et al. The feasibility of vibration as a tool to assess spinal integrity. J Biomech 2008;41(10):2319–23.

[17] Kawchuk GN, Decker C, Dolan R, et al. Structural health monitoring to detect the presence, location and magnitude of structural damage in cadaveric porcine spines. J Biomech 2009;42(2):109–15.

[18] Lin, RM, Tsai KH, Chang GL. Distribution and regional strength of trabecular bone in the porcine lumbar spine. Clin Biomech 1997;12(5):331–6.

[19] Marras WS. Occupational low back disorder causation and control. Ergonomics 2000;43(7):880–902.

[20] McBroom RJ, Hayes WC, Edwards WT, et al. Prediction of vertebral body compressive fracture using quantitative computed tomography. J Bone Joint Surg Am 1985;67(8):1206–14.

[21] Myers ER and Wilson SE. Biomechanics of osteoporosis and vertebral fracture. Spine 1997;22(24 Suppl):25S–31S.

[22] Nachemson A and Elfström G. Intravital dynamic pressure measurements in lumbar discs: a study of common movements, maneuvers and exercises. Scand J Rehabil Med Suppl 1970;1:1–40.

[23] Nachemson AL. Disc pressure measurements. Spine 1981;6(1):93–7.

[24] Panjabi MM, Andersson GB, Jorneus L, et al. In vivo measurements of spinal column vibrations. J Bone Joint Surg Am 1986;68(5):695–702.

[25] Panjabi MM, Krag MH, Chung TQ. Effects of disc injury on mechanical behavior of the human spine. Spine 1984;9(7):707–13.

[26] Parkinson RJ, Callaghan JP. The role of dynamic flexion in spine injury is altered by increasing dynamic load magnitude. Clin Biomech 2009;24(2):148–54.

[27] Polga DJ, Beaubien BP, Kallemeier PM, et al. Measurement of in vivo intradiscal pressure in healthy thoracic intervertebral discs. Spine 2004;29(12):1320–4.

[28] Pope MH, Wilder DG, Jorneus L, et al. The response of the seated human to sinusoidal vibration and impact. J Biomech Eng 1987;109(4):279–84.

[29] Rajasekaran S, Bajaj N, Tubaki V, et al. ISSLS Prize winner: The anatomy of failure in lumbar disc herniation: an in vivo, multimodal, prospective study of 181 subjects. Spine 2013;38(17):1491–500.

[30] Teo JCM, Si-Hoe KM, Keh JEL, et al. Correlation of cancellous bone microarchitectural parameters from microCT to CT number and bone mechanical properties. Mat Sci Eng C 2007;27(2):333–9.

[31] Teo JCM, Si-Hoe KM, Keh JEL, et al. Relationship between CT intensity, micro-architecture and mechanical properties of porcine vertebral cancellous bone. Clin Biomech 2006;21(3):235–44.

[32] Vernon-Roberts B and Pirie CJ. Healing trabecular microfractures in the bodies of lumbar vertebrae. Ann Rheum Dis 1973;32(5):406–12.

[33] Voloshin, A, and J Wosk. 1982. "An in vivo study of low back pain and shock absorption in the human locomotor system." Jour-

nal of biomechanics 15(1): 21-27
[34] Wilder DG, Woodworth BB, Frymoyer JW, et al. Vibration and the human spine. Spine 1982;7(3):243–54.
[35] Wilke HJ, Neef P, Caimi M, et al. New in vivo measurements of pressures in the intervertebral disc in daily life. Spine 1999;24(8):755–62.
[36] Yingling VR, Callaghan JP, McGill SM. The porcine cervical spine as a model of the human lumbar spine: an anatomical, geometric, and functional comparison. J Spinal Disord 1999;12(5):415–23.

Acknowledgements: We would like to thank the International Society of Biomechanics in the form of the Young Investigators Award, and the Natural Sciences and Engineering Research Council (NSERC), Canada

Financial support : Natural Sciences and Engineering Research Council (NSERC),Canada.

Conflict of Interest: None of the authors have a conflict of interest with information in this manuscript.